Classification of Sliding bifurcations in dry-friction oscillators

M. di Bernardo [*], P. Kowalczyk[*†], A. Nordmark[‡]

July 12, 2002

Abstract

Recent investigations of non-smooth dynamical systems led to the study of a class of novel bifurcations termed as *sliding bifurcations*. These bifurcations are a characteristic feature of so-called Filippov systems, i.e. systems of ODEs with discontinuous right-hand side. In this paper we show that sliding bifurcations also play an important role in organising the dynamics of dry friction oscillators, which constitute a subclass of non-smooth systems; non-smoothness being brought about by the character of friction law. After introducing the possible codimension-1 sliding bifurcations, we show that these bifurcations organise different types of "slip to stick-slip" transitions in the dry friction oscillators. In particular, we show both numerically and analytically that a sliding bifurcation is the mechanism causing the sudden jump to chaos often reported in the literature on friction systems. To analyse such bifurcation we make use of a new analytical method based on the study of appropriate normal form maps describing the sliding bifurcation. In so doing we explain under what circumstances the theory of so-called border-collision bifurcations can be used to explain the onset of complex behaviour in stick-slip systems.

1 Introduction

In Engineering friction plays an important role. It is the source of self-sustained oscillations termed stick-slip vibrations. These oscillations are often undesired effects observed in many areas of Engineering. Examples include torsional stick-slip vibrations in drill strings, squeaking doors and squealing railway wheels.
Thus, it is not surprising that systems with friction have been attracting the attention of scientists for decades [1, 2, 3]. Only in recent years, due to the introduction of new analytical techniques these systems have been studied from the standpoint of bifurcation theory.

In [4] Popp and Stelter introduce four different models including single-degree-of-freedom oscillator with external forcing where chaotic behaviour characterised by stick-slip motion is found. Moreover, they find different routes to chaos (intermittency, period-doubling) and different modes of stick-slip behaviour in their model problems. In [5] Stelter studies a simple beam system to determine how continuous structures behave under the action of dry friction forces.

[*]Department of Engineering Mathematics, University of Bristol BS8 1TR U.K. m.dibernardo@bristol.ac.uk

[†] *Corresponding Author.* Department of Engineering Mathematics, University of Bristol BS8 1TR U.K. Tel. +44(0)1179289798, fax +44(0)117 9251154 E-mail: p.kowalczyk@bristol.ac.uk

[‡]Department of Mechanics, Royal Institute of Technology, Sweden nordmark@mech.kth.se

Here, chaotic mode characterised by stick-slip motion is also found. In a further study, the bifurcation behaviour of a non-smooth friction oscillator under pure self and/or external excitation is treated [6, 7]. In the case of external excitation, the system is shown to exhibit a sensitive dependence on the bifurcation parameter, with a rich class of bifurcations being observed under parameter variations. The theoretical results were verified experimentally together with the bifurcation diagrams of the system for different types of excitation.

Work carried by Galvanetto addresses the problem of bifurcations in a two block stick-slip system [8, 9, 10, 11]. A one dimensional map is introduced for studying bifurcations in the four dimensional system. The bifurcation scenarios observed include a class of bifurcations leading to the onset of stick-slip motion. Non-standard bifurcations have also been detected in a simple damped oscillator [12].

Self-excited vibrating system with dry-friction were studied by Yoshitake and Sueoka in [13]. An interesting route to chaos is reported here. It is shown that a period doubling cascade is abruptly terminated by an outburst of chaotic behaviour due to the transition from slip to stick-slip motion. The authors conjecture that the onset of chaotic stick-slip vibrations is associated somehow to the occurrence of so-called border-collision bifurcations. These bifurcations can only be observed in dynamical systems with discontinuous non-linearities and have been shown to characterise the dynamics of a wide range of systems of relevance in applications [14, 15, 16, 17]. Border-collisions, for example, were shown to be fundamental in organising the dynamics of DC/DC converters in Power Electronics [18, 19, 20] walking mechanisms, and vibro-impacting mechanical systems [21]. One of the most common features of these bifurcations is the abrupt transition from a periodic to a chaotic solution. This is a very similar feature to the one reported in [13] for a friction oscillator which might lead to deduce that border-collisions are indeed at play also in friction systems.

This conjecture, though, proves hard to be characterised analytically as there is a fundamental problem recently outlined in [22, 23]. As shown in [22, 23], the theory of border-collisions can only be used to characterise the behaviour of continuous-time systems when a periodic orbit hits tangentially a non-smooth manifold or "corner" between phase space regions associated to different functional forms of the system under investigation. Only in this case the normal form map associated to the bifurcation event is piecewise linear and hence the classification strategy for bifurcations in piecewise linear maps can be used to characterise the transition observed in the continuous-time system. This is not the case in general for friction oscillators where the phase space discontinuity boundary associated to the Coulomb friction characteristics is a sufficiently smooth manifold (see Sec. 4 for further details).

The problem then is how to characterise and classify abrupt transitions, such as the one observed in [13] for a friction oscillator which (i) cannot be explained in terms of bifurcations also observed in smooth systems and (ii) involve a "slip to stick-slip" transition.

In this paper, we show that many of the bifurcations associated to the onset of stick-slip motion in friction oscillators can actually be explained in terms of a novel class of bifurcations, termed as *sliding bifurcations*, whose occurrence was independently reported in [24] and [25].

The starting point is to note that, as reported in [26], the stick phase in dry friction oscillators can be linked with the so-called *sliding mode* studied by Filippov [27] and Utkin [28]. Thus, periodic stick-slip motion in friction oscillators correspond to periodic orbits characterised by segments of sliding mode, or *sliding orbits* as they were recently termed in the literature [25]. In [29], it was shown that there are four distinct bifurcation scenarios termed as **sliding bifurcations** associated to the birth and bifurcations of an orbit with a sliding segment. Sliding bifurcations were shown to organise a variety of bifurcation scenarios including novel routes to chaos, sliding-adding scenarios and multisliding behaviour (for further details see [25]).

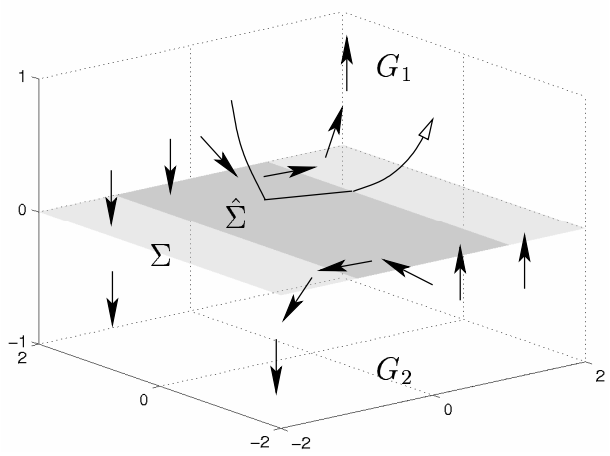

Figure 1: Phase space topology of a system with discontinuous vector fields

We propose that these four distinct scenarios can also explain *stick to stick-slip* transitions in dry-friction oscillators and bifurcations involving stick-slip periodic solutions. Recently, it has been shown that certain types of sliding bifurcations can be associated under certain conditions to piecewise-linear normal form maps [23]. Thus, as our analysis proves, the onset of stick-slip chaos in friction systems can be rigorously classified using the theory of border-collisions. Moreover, it can be shown that different types of sliding bifurcations are associated with different functional forms of their normal form maps. Therefore, we anticipate that they can be used to explain other bifurcation scenarios in friction oscillators which have been left unexplained in the literature.

The rest of the paper is outlined as follows. In the next section (Sec. 2) the phase space topology we are concerned with is introduced. Sliding bifurcations are defined and four distinct sliding bifurcation scenarios are presented. In Sec. 4 the dry friction oscillator studied in [13] is studied and shown to exhibit the so-called grazing-sliding bifurcation. In the following section, an analytical method to studying periodic orbits undergoing a grazing-sliding bifurcation is detailed. A discussion of the possible dynamical scenarios and how to classify them is also included. In Sec. 5, the grazing-sliding bifurcation in the system of interest is examined using analytical tools introduced in Sec. 3.1. Finally in Sec. 6, conclusions are drawn.

2 Sliding Bifurcations: an overview

2.1 Phase Space Topology

We focus our attention to systems with discontinuous vector fields. Such systems are characterised by the presence of discontinuity boundaries in phase space between regions where the vector field is smooth and continuous. We consider a sufficiently small region $D \subset R^n$ of phase space where the equations governing the system flow can be written as:

$$\dot{x} = \begin{cases} F_1(x,\mu) & \text{for} \quad H(x) > 0, \\ F_2(x,\mu) & \text{for} \quad H(x) < 0, \end{cases} \tag{1}$$

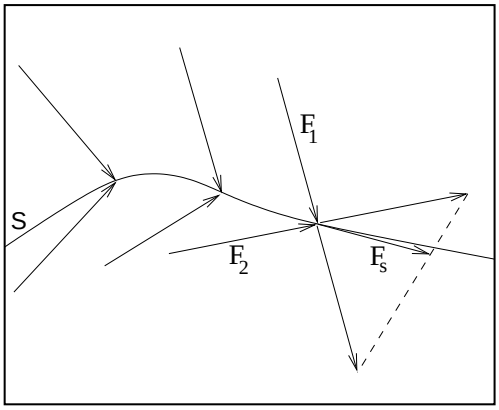

Figure 2: Geometrical construction of the vector field F_s, which governs the flow within a system discontinuity set Σ

where F_1, F_2 are sufficiently smooth vector functions and $H(x)$ is some scalar function depending on the system states. D is split into two subspaces, say G_1 and G_2, with smooth and continuous dynamics. The discontinuity boundary between G_1 and G_2 we assume to be a smooth hyperplane, say Σ. Namely:

$$G_1 := \{x \in R^n : H(x) > 0\}, \tag{2}$$

$$G_2 := \{x \in R^n : H(x) < 0\}. \tag{3}$$

$$\Sigma := \{x \in R^n : H(x) = 0\}. \tag{4}$$

The resulting topology in the case of a three-dimensional vector field is shown schematically in Fig. 1. If the vector field points towards Σ from both subspaces G_1 and G_2, a trajectory hitting Σ is forced to evolve within the discontinuity set until reaching some point on it where one of the two vector fields, F_1 or F_2, changes its direction (the boundary of the shaded region in Fig. 1 denoted by $\hat{\Sigma}$). The solution which lies within the system discontinuity set is termed as sliding motion and the region of the discontinuity set where such a motion may occur is labelled *sliding region*. Throughout this region the following condition must hold:

$$\langle \nabla H, F_2 \rangle - \langle \nabla H, F_1 \rangle > 0, \tag{5}$$

where ∇H denotes a vector which is normal to Σ and $\langle \nabla H, F_i \rangle$ denotes the component of the vector field F_i along the normal to Σ.

Following Utkin's equivalent control method [28], we can derive the vector field F_s, which governs the flow within the sliding region, as a vector function belonging to the convex hull of F_1 and F_2:

$$F_s = \frac{F_1 + F_2}{2} + H_u \frac{F_2 - F_1}{2}, \tag{6}$$

where $-1 \leq H_u \leq 1$. $H_u(x)$ can be obtained in terms of F_1 and F_2 by considering that F_s must be tangential to the switching manifold, i.e. $\langle \nabla H, F_s \rangle = 0$.

Using this condition, we have

$$H_u(x) = -\frac{\langle \nabla H, F_1 \rangle + \langle \nabla H, F_2 \rangle}{\langle \nabla H, F_2 \rangle - \langle \nabla H, F_1 \rangle}. \tag{7}$$

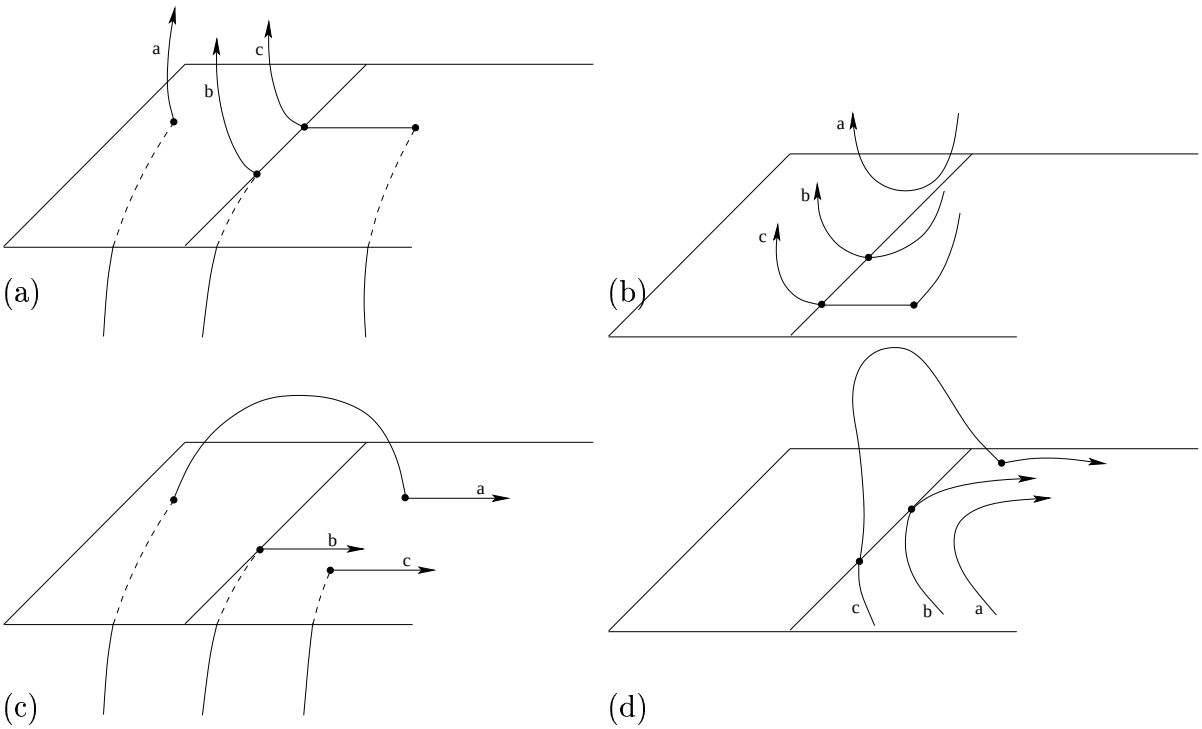

Figure 3: The four possible bifurcation scenarios involving collision of a segment of the trajectory with the boundary of the sliding region

Note that Utkin's method is derived from straightforward geometric considerations as illustrated by Fig. 2. In particular, the sliding vector field is obtained by considering a vector function tangential to the switching manifold. Using this function, we can now define the sliding region as:

$$\hat{\Sigma} := \{x \in \Sigma : |H_u(x)| < 1\}, \tag{8}$$

and its boundaries:

$$\partial\hat{\Sigma}^- := \{x \in \Sigma : H_u(x) = -1\}, \tag{9}$$

$$\partial\hat{\Sigma}^+ := \{x \in \Sigma : H_u(x) = 1\}. \tag{10}$$

2.2 The four possible cases

We define sliding bifurcations as bifurcations due to interactions between a system periodic solution and the boundary of the sliding region $\partial\hat{\Sigma}^{\pm}$. Following [24, 29, 30] we can distinguish four possible bifurcation scenarios involving sliding (see Fig. 3). Figure 3-(a) depicts the scenario we term as **sliding bifurcation of type I**. Under parameter variations, a piece of a trajectory (denoted by a letter b in 3-(a)) hits the boundary of the sliding region. Further variation of the parameters causes the trajectory to hit Σ within $\hat{\Sigma}$, yielding the formation of an additional segment of the trajectory lying within the system discontinuity set (see in Fig. 3-(a) trajectory c).

In the case presented in Fig. 3-(b), instead, a section of trajectory lying in region G_1 or G_2 grazes the boundary of the sliding region from above (or below). Again, this causes the formation of a section of sliding motion. This bifurcation is termed as grazing-sliding bifurcation and as will be shown later in the paper it may cause a sudden jump to chaos.

BIFURCATION	sliding I	grazing-sliding	sliding II	multisliding
CONDITION 1	$H(\mathbf{x}^*)=0,\ \nabla H(\mathbf{x}^*)\neq 0$			
CONDITION 2	$H_u(\mathbf{x}^*)=-1,\ \Leftrightarrow F_s=F_1 \Leftrightarrow \langle \nabla H, F_1\rangle = 0$ at $\mathbf{x}^*$			
CONDITION 3	$\langle \nabla H, \frac{\partial F_1}{\partial x}F_1\rangle > 0$		$\langle \nabla H, \frac{\partial F_1}{\partial x}F_1\rangle < 0$	$\langle \nabla H, \frac{\partial F_1}{\partial x}F_1\rangle = 0$
CONDITION 4	no condition defined			$\langle \nabla H, \left(\frac{\partial F_1}{\partial x}\right)^2 F_1\rangle < 0$

Table 1: Analytical conditions for sliding bifurcations

A different bifurcation event, which we shall call **sliding bifurcation of type II** or switching-sliding, is depicted in Fig. 3-(c). This scenario is similar to the sliding bifurcation of type I shown in Fig. 3-(a). We see a section of the trajectory crossing transversally the boundary of the sliding region. Now, though, the trajectory stays locally within the sliding region instead of zooming off the switching manifold Σ.

The fourth and last case is the so-called **multisliding bifurcation**, shown in Fig. 3-(d). It differs from the scenarios presented above since the segment of the trajectory which undergoes the bifurcation lies entirely within the sliding region $\hat{\Sigma}$. Namely, as parameters are varied, a sliding section of the system trajectory hits tangentially (grazes) the boundary of the sliding region. Further variations of the parameter cause the formation of an additional segment of trajectory lying above or below the switching manifold, i.e. in region G_1 or G_2.

To each of these four scenarios, we can associate a set of analytical conditions describing the system properties at the bifurcation point [30]. These are summarised in Table 1.

3 Classification of sliding bifurcations

Once a bifurcation event has been detected in a system of interest, a fundamental problem is to predict the dynamical scenario associated with it. For example, when bifurcations in smooth systems are considered, the derivation of appropriate normal forms allows the classification of different bifurcation types such as saddle-nodes, Hopf and period-doublings [31]. As shown in [30] and discussed above, piecewise smooth systems exhibit bifurcations, such as those involving sliding, which cannot be classified using standard techniques. In particular, the same bifurcation event can be associated to different dynamical scenarios according to the properties of the system vector field locally to the bifurcation point.

Recently, a new classification strategy has been proposed to identify the dynamical scenarios due to the onset of a sliding bifurcation, and more generally a *non-standard* bifurcation in piecewise smooth systems. To illustrate the methodology we take as a representative example the case of a periodic orbit undergoing a grazing-sliding bifurcation such as the one depicted in Fig. 2(b). A similar procedure can be used to classify other types of sliding bifurcations.

3.1 The Grazing-Sliding case

For the sake of clarity, we consider the simplest possible scenario for a periodic orbit to undergo a grazing-sliding bifurcation. Namely, we consider the periodic orbit, shown in Fig.4, that goes through a point A on the boundary of the sliding region $\hat{\Sigma}$ satisfying conditions for this case,

but otherwise lying entirely in region G_1.

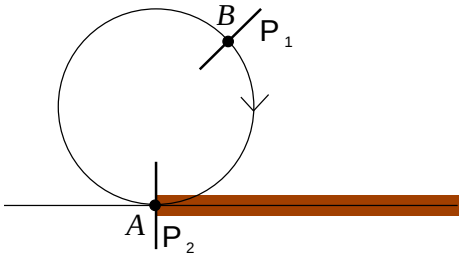

Figure 4: Simplest orbit undergoing grazing-sliding bifurcation

To study stability and bifurcations, we then consider a section Π_1 transversal to the flow in region G_1 and a section $\Pi_2 := \{x \in R^n : H_u(x) = -1\}$ going through point A transversal to flow ϕ_1. The full Poincaré map, P, maps Π_1 back to itself and is obtained by composition of the following mappings:

- $P_{12} : \Pi_1 \mapsto \Pi_2$,
- $P_{22} : \Pi_2 \mapsto \Pi_2$,
- $P_{21} : \Pi_2 \mapsto \Pi_1$.

Note that P_{12} and P_{21} are smooth maps and of full rank since they are obtained from the flow ϕ_1, i.e. by considering the system evolution in region G_1. The mapping P_{22}, instead, is the one whose effect is to take into account the presence along the trajectory of the sliding region. In particular, such mapping is simply the identity if the trajectory does not interact with the sliding region (i.e. before the bifurcation event) while introduces a discontinuity otherwise. In order to classify the dynamical scenarios following a grazing-sliding we then need to:

1. derive the analytical form of the mapping P_{22} (the discontinuity map);
2. study the dynamics of the Poincaré map of the bifurcating orbit.

It is worth mentioning here that, as recently shown in [30], the functional form of the discontinuity map depends uniquely on the bifurcation type considered and can be obtained in closed form through a combination of asymptotics and Taylor series expansion.

Note that in the case of periodically forced systems the discontinuity map P_{22} and mappings P_{12}, P_{22} correspond to "parts of" a stroboscopic map. Hence, the correction brought about by the discontinuity map should be such that the period of the orbit remains uperturbed. In this case P_{22} is often termed as a zero-time discontinuity map or ZDM.

In the case of non-periodically forced systems or when the introduction of a stroboscopic map is not possible, the ZDM needs to be composed with some projection mapping M, which maps the correction back to section Π_2. The composition of the ZDM and the projection mapping M is then referred to as a Poincaré Discontinuity Mapping or PDM.

In what follows, we outline briefly the derivation of the ZDM for the grazing-sliding bifurcation under investigation. This will be used later in Sec. 4 to characterise the complex behaviour of a dry-friction oscillator. (More details about the methodology used is presented in [30], where the derivation of normal form maps for all types of sliding bifurcations can be found.)

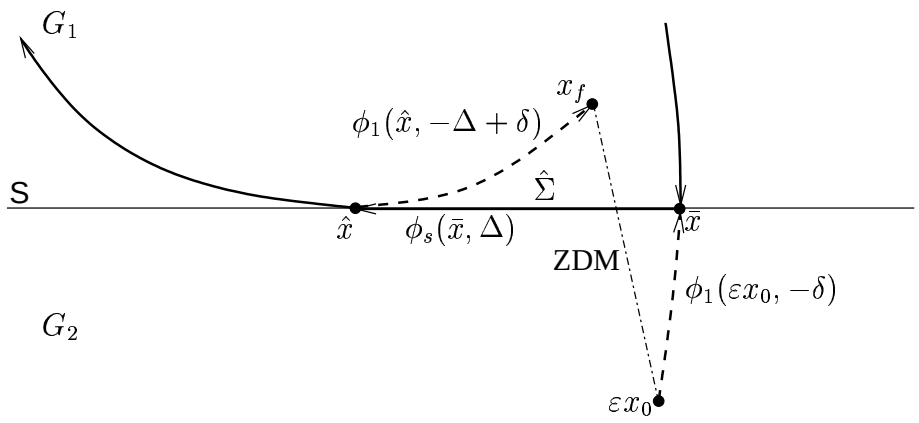

Figure 5: Schematic representation of constructing the ZDM for the case of grazing sliding bifurcation

3.1.1 The Grazing-Sliding Discontinuity Map

The key to derive the normal form map of a grazing-sliding bifurcation is to use the idea recently introduced in [32]. This is graphically sketched in Fig. 5 where the periodic orbit is shown after the grazing-sliding bifurcation and therefore contains a sliding segment (denoted by a solid line joining $\bar{x}$ and $\hat{x}$ points).

Namely, there are two alternative ways of describing the evolution of the sliding orbit in Fig. 5. The first is to use flow ϕ_1 until reaching the sliding region (point $\hat{x}$), switching then to the natural, sliding flow ϕ_s, until the trajectory reaches the boundary of $\hat{\Sigma}$ when flow ϕ_1 is used again.

The other way to describe the orbit shown in Fig. 5 is to use flow ϕ_1 all way through (even if the orbit crosses the sliding region), applying an appropriate correction at an intermediate point to account for the presence of the sliding region. Such a correction is actually the discontinuity map and contains all the crucial information concerning the influence of the sliding region on the evolving trajectory (the map from x_0 to x_1 in Fig. 5).

To construct an analytical approximation of the ZDM, the methodology presented in [30] can be used. This is based on three different steps: (i) firstly, we consider the evolution of the trajectory from the point x_0 backward in time to the point $\bar{x} \in \hat{\Sigma}$; (ii) we then study the sliding motion from $\bar{x}$ to the boundary of the sliding region (point $\hat{x}$) (iii) finally, we consider the evolution along ϕ_1 from the point $\hat{x}$ to some final point x_1. In so doing, we require that the elapsed time to get from the point x_0 to x_1 is equal to 0. Note that the final point x_1 does not lie on the boundary of the sliding region (section Π_2 in Fig. 4) since it is evaluated from $\hat{x}$ following flow ϕ_1.

Using a combination of Taylor series expansion and asymptotics (as detailed in [30]), it can be shown that the grazing-sliding bifurcation is associated to leading-order to the following discontinuity map (P_{22}):

$$x_1 = D(x_0) = \begin{cases} x_0 & \text{if } \langle \nabla H, x_0 \rangle \geq 0 \\ x_0 - \dfrac{\langle \nabla H, x_0 \rangle}{\langle \nabla H, F_2 \rangle}(F_2 - F_1) + \mathcal{O}(\varepsilon^{3/2}) & \text{if } \langle \nabla H, x_0 \rangle < 0 \end{cases}, \tag{11}$$

Note that (11) is the identity below the sliding region (region G_1) and contains a linear leading-order term otherwise.

From (11) we see that the correction brought about by the ZDM, in the grazing-sliding case cannot be parallel to the vector field F_1, as it has the direction of $(F_2 - F_1)$. If, in fact, $(F_2 - F_1)$ were parallel to F_1, then sliding would not be possible. Hence, when non-stroboscopic mapping are considered, the composition of the ZDM with the projection map M does not cancel out the leading-order term and the discontinuity is still of linear order.

From what mentioned above, the derivative of the Poincaré map P describing the periodic orbit is discontinuous at the bifurcation point. Naturally the same holds true for the stroboscopic map composed directly with the ZDM for grazing-sliding. Thus, for such mappings we cannot conclude that the periodic orbit will persist under parameter variations that would force it to acquire a sliding portion. To classify the bifurcation scenarios following a grazing-sliding event, one should therefore refer to the literature concerning border-collision bifurcations in piecewise-linear maps [14, 15, 33] (see Sec. 5 for further details).

Finally, if the orbit survives the bifurcation, we can expect a jump in eigenvalues as the periodic orbit acquires a sliding portion. The jump in eigenvalues is nicely illustrated by the fact that a sliding periodic orbit must have at least one eigenvalue 0, whereas no such restriction exists for an orbit lying entirely in region G_1.

3.2 Discontinuity maps of other sliding bifurcations

As shown in [30], other types of sliding bifurcations in general are associated with discontinuity maps of the form :

$$x \mapsto \begin{cases} A_1 x + B\mu, & \text{if } c^T x < 0 \\ A_2 x + D(c^T x)^\gamma + B\mu, & \text{if } c^T x > 0. \end{cases} \tag{12}$$

where A_1, A_2, B, c^T and D are appropriate matrices and:

- $\gamma = 1$ in the grazing-sliding case (scenario (b) in Fig. 3);
- $\gamma = 2$ in the multisliding case ((scenario (d) in Fig. 3);
- $\gamma = 2$ in the sliding bifurcation type I (scenario (a) in Fig. 3);
- $\gamma = 3$ in the sliding bifurcation type II (scenario (c) in Fig. 3)

Normal form maps are therefore characterised by different nonlinearities according to the bifurcation scenario they describe. Piecewise-linear normal form maps are only associated to the grazing-sliding case.

4 Sliding Bifurcations in Dry Friction Oscillators

As anticipated in the introduction, the stick phase of the dynamics of friction oscillators can be analysed as a segment of sliding motion [26]. Thus, the sliding bifurcation scenarios presented in the previous section are likely to occur in this important class of dynamical systems and can be used to explain the complex dynamics often reported in the literature.

Evidence to support this conjecture can be found in [7], where a class of friction oscillators is subject to an extensive experimental and numerical investigation. The oscillator studied therein exhibits transitions from periodic orbits without any stick phase to periodic orbits characterised

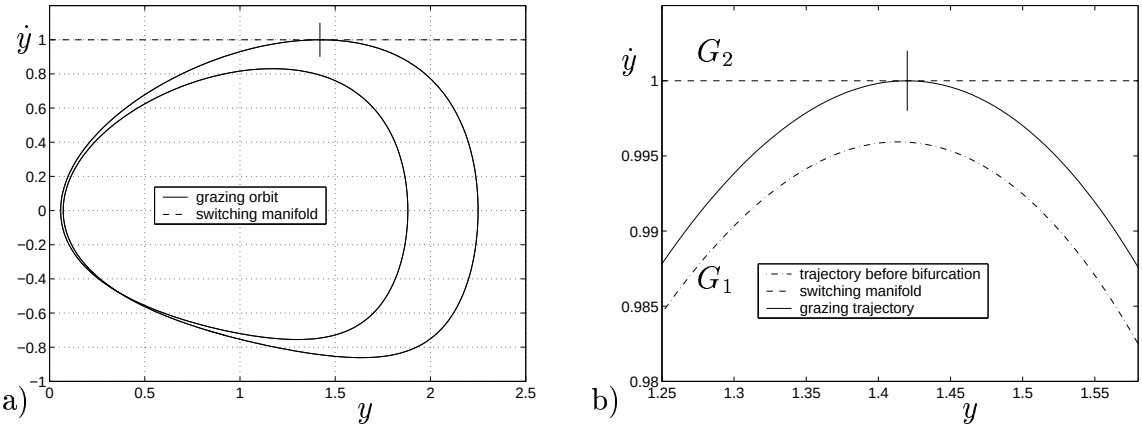

Figure 6: Orbit of the period $4T$ undergoing grazing-sliding bifurcation for $\nu = 1.7077997$ (a); Zoom of the region where grazing-sliding occurs - segment of an orbit at and before the bifurcation (b). The dash-dotted segment correspond to the periodic orbit for $\nu = 1.7082$ that clearly does not reach the switching manifold. Variation of the parameter ν below 1.7077997 causes the birth of aperiodic mode of stick-slip motion.

by one or more stick phases per period. In view of our results, such transition can be classified as a sliding bifurcation type I. The formation of an orbit characterised by a multiple number of stick phases per period observed in the paper clearly indicates the occurrence of a cascade of sliding bifurcations.

A more intriguing scenario is exhibited by the dry friction oscillator studied in [13], which is numerically shown to exhibit a route to chaos characterised by the abrupt transition from slip periodic motion to stick-slip chaotic behaviour. The bifurcation mechanism causing the onset of such aperiodic motion is left unexplained by the authors who conjecture that it must be due to some type of non-smooth bifurcation without offering any analytical explanation.

In what follows we will use the theory of sliding bifurcations and their normal form maps to unfold this bifurcation scenario. We will use the oscillator presented in [13] as an illustrative example to propose sliding bifurcations as a fundamental mechanism in organising the dynamics of friction oscillators.

Following [13], the dry friction oscillator under investigation in the dimensionless form can be expressed as:

$$\ddot{y} + y = f(1 - \dot{y}) + F\cos(\nu t), \tag{13}$$

where:

$$f(1 - \dot{y}) = \alpha_0 \mathrm{sgn}(1 - \dot{y}) - \alpha_1(1 - \dot{y}) + \alpha_2(1 - \dot{y})^3 \tag{14}$$

is a kinematic friction characteristic and $1 - \dot{y}$ corresponds to a relative velocity between the driving belt and moving block. In the case when $1 - \dot{y} = 0$ the relative velocity is 0 and the kinematic friction is set valued i.e.: $-\alpha_0 < f(1 - \dot{y}) < \alpha_0$. The coefficients of the kinematic friction characteristic i.e.: α_0, α_1, α_2 are positive constants. F is an amplitude, ν a normalised angular velocity and T a period of the forcing term.

An extensive numerical study of the aforementioned oscillator allowed the detection of various dynamical scenarios including incomplete period doubling cascade, abrupt transitions to chaos and different modes of subharmonic motion (for details we refer the reader to [13]).

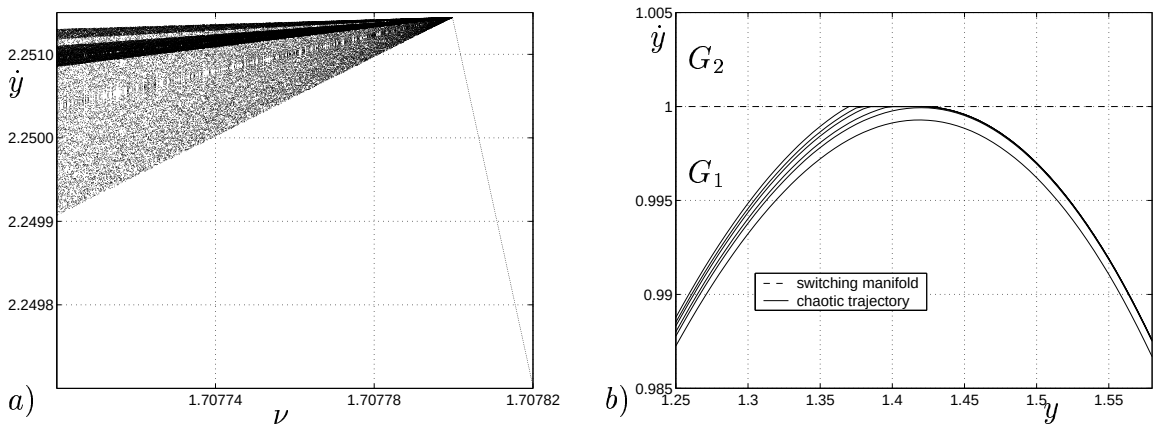

Figure 7: Bifurcation diagram obtained from the numerical integration of the system under consideration (a) and a period chaotic trajectory in the neighbourhood of the switching manifold.

We focus, in particular, on the bifurcation scenario giving rise to the sudden emergence of chaotic stick-slip motion shown in Fig. 6(a). The bifurcation was detected for parameter values $\alpha_0 = 1.5$, $\alpha_1 = 1.5$, $\alpha_2 = 0.45$, $F = 0.1$, under variation of the bifurcation parameter ν in a neighbourhood of $\nu = 1.7078$. As shown in Fig. 6(a), at the bifurcation point, a $4T$-periodic orbit grazes the switching manifold at the boundary of the sliding region (denoted in the figure by a short vertical line) for $\nu = 1.7077997$. According to what mentioned earlier in the paper, the observed scenario corresponds to a grazing-sliding bifurcation, as the bifurcating orbit grazes from below the boundary of the region where stick motion can take place. This can be more clearly seen in Fig. 6(b).

The existence of a chaotic attractor for $\nu < 1.7077997$ was confirmed by computing the Lyapunov exponents as reported in [13]. As shown in Fig. 7(b) the chaotic motion is characterised by stick-slip motion.

Using the analytical approach presented in the previous sections, we will now try to characterise these numerical results by carrying out an appropriate analysis of the system at the bifurcation point.

We start by putting system (13) under consideration in the general form (1). Setting $\nu t = \tau$, $x_1 = y$, $x_2 = \dot{y}$, we can express (13) as a set of first order ODE's with discontinuous right-hand side of the form:

$$\dot{x}_1 = x_2, \tag{15}$$

$$\dot{x}_2 = -x_1 + \alpha_0 \mathrm{sgn}(1 - x_2) - \alpha_1(1 - x_2) + \alpha_2(1 - x_2)^3 + F\cos(\tau), \tag{16}$$

$$\dot{\tau} = \nu. \tag{17}$$

The switching surface Σ, in this case can be defined as:

$$\Sigma := \{\mathbf{x} \in R^3 : H(\mathbf{x}) = 1 - x_2 = 0\}, \tag{18}$$

where $\mathbf{x} = \begin{bmatrix} x_1 & x_2 & \tau \end{bmatrix}^T$ and $H(\mathbf{x}) = 1 - x_2$ is a scalar function defining the switching manifold.

Thus, the normal to Σ is the vector:

$$\nabla H = \begin{bmatrix} 0 & -1 & 0 \end{bmatrix}. \tag{19}$$

The dynamics of the system is smooth and continuous when $H(\mathbf{x})$ is non-zero and is governed by the vector fields:

$$F_1 = \begin{pmatrix} x_2 \\ -x_1 + \alpha_0 - \alpha_1(1-x_2) + \alpha_2(1-x_2)^3 + F\cos(\tau) \\ \nu \end{pmatrix} \qquad \text{when } H(\mathbf{x}) > 0 \tag{20}$$

and

$$F_2 = \begin{pmatrix} x_2 \\ -x_1 - \alpha_0 - \alpha_1(1-x_2) + \alpha_2(1-x_2)^3 + F\cos(\tau) \\ \nu \end{pmatrix} \qquad \text{when } H(\mathbf{x}) < 0 \tag{21}$$

According to our analysis, sliding motion (stick) is possible if condition (5) is satisfied, i.e. if:

$$\alpha_0 > 0 \tag{22}$$

The condition above holds true since it is assumed that the coefficients of the kinematic friction characteristic (14) are positive.

Using Utkin's equivalent control method we can define the vector field F_s which governs the flow on the switching manifold, as described in (6). Substituting (20) and (21) into (6), we then get the following expression for the sliding flow F_s :

$$F_s = \begin{pmatrix} x_2 \\ -x_1 - \alpha_1(1-x_2) + \alpha_2(1-x_2)^3 + F\cos(\tau) - H_u(\mathbf{x})\alpha_0 \\ \nu \end{pmatrix} \tag{23}$$

where $-1 < H_u(x) < 1$. Since, the vector field F_s must lie on the switching manifold Σ, we have:

$$\langle \nabla H, F_s \rangle = 0, \tag{24}$$

and using (7), we can express $H_u(\mathbf{x})$ as:

$$H_u(\mathbf{x}) = -\frac{x_1 + \alpha_1(1-x_2) - \alpha_2(1-x_2)^3 - F\cos(\tau)}{\alpha_0}. \tag{25}$$

The sliding region $\hat{\Sigma}$ can then be defined as:

$$\hat{\Sigma} = \{\mathbf{x} \in \Sigma : -1 \leq \frac{-x_1 + F\cos(\tau)}{\alpha_0} \leq 1\}. \tag{26}$$

To carry out the analytical investigation of the bifurcation point under consideration, it is useful to assume that the bifurcation point $\mathbf{x}^*$ occurs at the origin. Since, in our case the bifurcation point is $\begin{pmatrix} x_1^* & x_2^* & \tau^* \end{pmatrix} = \begin{pmatrix} \alpha_0 + F\cos(\tau^*) & 1 & \tau^* \end{pmatrix} = \begin{pmatrix} 1.4198660038 & 1 & 3.7828571553 \end{pmatrix}$ we consider an appropriate translation of the system coordinates. Namely, we choose the new set of local coordinates as $\tilde{x}_1 = x_1 - x_1^*$, $\tilde{x}_2 = x_2 - x_2^*$, $\tilde{\tau} = \tau - \tau^*$. Under this choice of coordinates, the vector fields F_1, F_2 and F_s become:

$$\tilde{F}_1 = \begin{pmatrix} 1 + \tilde{x}_2 \\ f_2 \\ \nu \end{pmatrix}, \tag{27}$$

$$\tilde{F}_2 = \begin{pmatrix} 1+\tilde{x}_2 \\ -2\alpha_0 + f_2 \\ \nu \end{pmatrix}, \tag{28}$$

and

$$\tilde{F}_s = \begin{pmatrix} 1+\tilde{x}_2 \\ 0 \\ \nu \end{pmatrix}, \tag{29}$$

where

$$f_2 = -\tilde{x}_1 + \alpha_1 \tilde{x}_2 - \alpha_2 \tilde{x}_2^3 + F\left(\cos(\tau^* + \tilde{\tau}) - \cos(\tau^*)\right). \tag{30}$$

Similarly, we obtain the functions $\tilde{H}$ and $\tilde{H}_u$ as:

$$\tilde{H}(\tilde{\mathbf{x}}) = -\tilde{x}_2, \tag{31}$$

$$\tilde{H}_u(\tilde{\mathbf{x}}) = -1 + \frac{f_2}{\alpha_0}. \tag{32}$$

By definition the bifurcation point in a new set of coordinates is translated to the origin i.e.: $\begin{pmatrix} \tilde{x}_1^* & \tilde{x}_2^* & \tilde{x}_3^* \end{pmatrix} = \begin{pmatrix} 0 & 0 & 0 \end{pmatrix}$ therefore, we can write:

$$\tilde{F}_1(0) = \tilde{F}_s(0) = \begin{pmatrix} x_2^* \\ 0 \\ \nu \end{pmatrix}. \tag{33}$$

We can now check that the set of analytical conditions which identify a grazing-sliding bifurcations (see Tab. 1) are indeed satisfied at the bifurcation point under investigation. In fact, we get:

1. $\tilde{H}(0) = 0$,
2. $\tilde{H}_u(0) = -1$,
3. $\langle \nabla \tilde{H}, \frac{\partial \tilde{F}_1}{\partial \mathbf{x}} \tilde{F}_1 \rangle = 1 + \nu F \sin(\tau^*) = 0.8971661 > 0$.

Thus, at the aforementioned value of x^*, the system satisfies all three conditions and it is therefore proven that the bifurcation event described in [13] is indeed due to a grazing-sliding bifurcation. We now show how knowledge of this can be used to classify analytically the observed bifurcation scenario and hence explain the sudden appearance of a chaotic attractor using the theory of border-collisions.

5 Explaining the onset of chaotic behaviour

5.1 Classification of grazing-sliding: the discontinuity map

Following the analysis introduced in the previous section, the first step to characterise the occurrence of the grazing-sliding bifurcation detected in the friction oscillator of interest (see Fig. 6)

is to derive an appropriate Poincaré mapping describing the bifurcating solution. In our case, we have a forced dynamical system with the bifurcating orbit being of period $4T$, i.e. four times the period T of the external forcing. Thus, the natural Poincaré map is a $4T$-stroboscopic mapping, say P_{4T}, which we assume to be affine and well represented by its linear terms, i.e.

$$P_{4T} : \tilde{\mathbf{x}}_{n+1} = A\tilde{\mathbf{x}}_n + B\tilde{\nu} = \begin{pmatrix} a_{11} & a_{12} \\ a_{21} & a_{22} \end{pmatrix} \tilde{\mathbf{x}}_n + \begin{pmatrix} b_1 \\ b_2 \end{pmatrix} \tilde{\nu} \tag{34}$$

where $\tilde{\mathbf{x}}_n$ is the two-dimensional state vector $\tilde{x}_n = \begin{bmatrix} \tilde{x}_{1n} & \tilde{x}_{2n} \end{bmatrix}^T$ and $\nu = \tilde{\nu} + \nu^*$ with $\nu^* = 1.7077997$, obtained by sampling the system states at time instants multiples of $4T$.

Note that we assume the map to be affine and sufficiently smooth away from the bifurcation point, i.e. when the orbit does not contain any segment of sliding (stick) motion. Smoothness is lost under parameter variation as the orbit grazes and then enters the sliding region.

For the $4T$ periodic orbit of interest computed earlier when $\nu^* = 1.7077997$, we find that:

$$\begin{aligned} a_{11} &= \frac{\partial \tilde{x}_{1n+1}}{\partial \tilde{x}_{1n}} = -1.85, \quad a_{12} = \frac{\partial \tilde{x}_{1n+1}}{\partial \tilde{x}_2 n} = 4.396, \quad a_{21} = \frac{\partial \tilde{x}_{2n+1}}{\partial \tilde{x}_1 n} = -1.14, \\ a_{22} &= \frac{\partial \tilde{x}_{2n+1}}{\partial \tilde{x}_2 n} = 2.704, \quad b_1 = \frac{\partial \tilde{x}_{1n+1}}{\partial \nu} = 4.498 \quad b_2 = \frac{\partial \tilde{x}_{2n+1}}{\partial \nu} = -1.755 \end{aligned} \tag{35}$$

The coefficients of matrices A and B shown above can be obtained numerically by considering small perturbations of each component of vector $\tilde{\mathbf{x}}$ and parameter ν while the other components and parameters are kept fixed. Note, that the matrix A involved is nonsingular, which is all that is required for the linear approximation to be valid.

To capture the influence of the grazing-sliding event, according to what presented above, we then need to compose (34) with the normal-form map for grazing-sliding given by (11). In the case of the friction oscillator (13) under discussion, this mapping takes the form:

$$D(\tilde{\mathbf{x}}_n) = \begin{cases} \tilde{\mathbf{x}}_n & \text{if} \quad \langle \nabla \tilde{H}, \tilde{\mathbf{x}}_n \rangle \geq 0, \\ \tilde{\mathbf{x}}_n - \dfrac{\langle \nabla \tilde{H}, \tilde{\mathbf{x}}_n \rangle}{\langle \nabla \tilde{H}, \tilde{F}_2 \rangle} (\tilde{F}_2 - \tilde{F}_1) & \text{if} \quad \langle \nabla \tilde{H}, \tilde{\mathbf{x}} \rangle < 0, \end{cases} \tag{36}$$

Substituting (19), (27), (28) for $\nabla \tilde{H}$, $\tilde{F}_1$, $\tilde{F}_2$ respectively and considering that the state variables of interest are x_1 and x_2, (36) becomes:

$$D(\tilde{\mathbf{x}}_n) = \begin{cases} \tilde{\mathbf{x}}_n & \text{if} \quad \tilde{x}_{2n} < 0, \\ \tilde{\mathbf{x}}_n + C\tilde{\mathbf{x}}_n & \text{if} \quad \tilde{x}_{2n} > 0. \end{cases} \tag{37}$$

where $C = \begin{pmatrix} 0 & 0 \\ 0 & -1 \end{pmatrix}$. To obtain the complete Poincaré mapping describing the orbit close to the bifurcation point, we now compose (37) with (34). Hence, we get that such Poincaré map is given by:

$$\tilde{\mathbf{x}}_{n+1} = \begin{cases} A_1\tilde{\mathbf{x}}_n + B\tilde{\nu} & \text{if} \quad \tilde{x}_{2n} < 0, \\ A_2\tilde{\mathbf{x}}_n + B\tilde{\nu} & \text{if} \quad \tilde{x}_{2n} > 0, \end{cases} \tag{38}$$

where $A_1 = A$ and $A_2 = A + AC$; or equivalently,

$$\tilde{\mathbf{x}}_{n+1} = \begin{cases} \begin{pmatrix} a_{11} & a_{12} \\ a_{21} & a_{22} \end{pmatrix} \tilde{\mathbf{x}}_n + \begin{pmatrix} b_1 \\ b_2 \end{pmatrix} \tilde{\nu} & \text{if} \quad \tilde{x}_{2n} < 0, \\ \begin{pmatrix} a_{11} & 0 \\ a_{21} & 0 \end{pmatrix} \tilde{\mathbf{x}}_n + \begin{pmatrix} b_1 \\ b_2 \end{pmatrix} \tilde{\nu} & \text{if} \quad \tilde{x}_{2n} > 0. \end{cases} \tag{39}$$

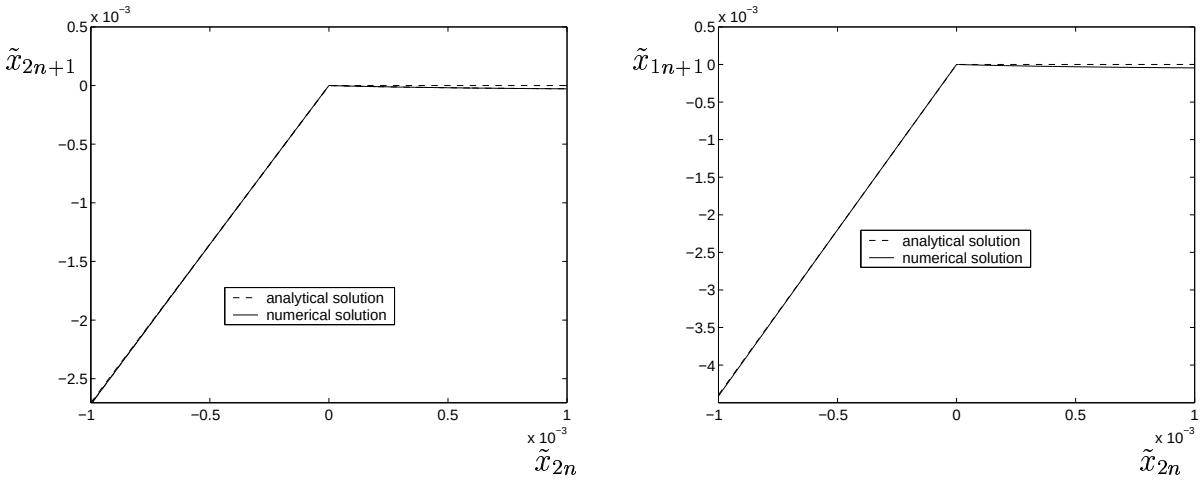

Figure 8: Numerical and analytical mappings at the bifurcation value of the control parameter ν

The comparison between a map obtained numerically and between the analytical mapping (39) is shown in Fig. 8. The figure depicts one dimensional projections of the 2-dimensional mapping (39). Coordiantes $\tilde{x}_{1n+1}$ and $\tilde{x}_{2n+1}$ are plotted versus $\tilde{x}_{2n}$ with $\tilde{x}_{1n} \equiv 0 \ \forall n$.

It is worth mentioning here that to retrieve a map obtained from numerical simulations of a system under consideration the stroboscopic map needs to be aplied at some value of $\tilde{x}_1$, say $\tilde{x}_1 \equiv \tilde{x}_{10} \ \forall n$ such that $\tilde{x}_{10} \neq 0$ but is applied at the close neighbourhood of 0.

The stroboscopic mapping of the bifurcating orbit has a piece-wise linear functional form (39). Hence the grazing sliding of the periodic solution under investigation correspond to a so-called border-collision of its corresponding map. In practice, as the periodic orbit hits tangentially the boundary of the sliding region (grazing sliding), the associated fixed point of map (39) crosses the boundary $\tilde{x}_2 = 0$ across which the map takes two different functional forms.

5.2 Classification of grazing-sliding: border-collision scenario

To predict and classify the scenario exhibited by the system past the bifurcation point, we can now use the classification scheme for border-collision bifurcations in piecewise-linear maps recently proposed in [33]. According to this strategy, to predict analytically the dynamical behaviour of the system at the grazing-sliding bifurcation, one needs to count the number of real eigenvalues of map (39) on both sides of the discontinuity boundary i.e.: for $\tilde{x}_{2n} < 0$ and $\tilde{x}_{2n} > 0$. Namely, we denote by σ_1^+ and σ_2^+ the number of real eigenvalues greater than 1 of matrices A_1 and A_2 respectively in equation (38). Similarly, we term σ_1^-, σ_2^- the number of real eigenvalues lower than -1 of the same matrices.

It is then possible to show that using these quantities, one can classify among the three following simplest scenarios (see [33] for further details).

1. **Border-crossing:** if $\sigma_1^+ + \sigma_2^+$ is even, the bifurcating orbit (without any stick phase) will simply change into an orbit characterised by a sliding segment of the same periodicity (i.e. a stick-slip periodic motion);

2. **Nonsmooth saddle-node:** if $\sigma_1^+ + \sigma_2^+$ is odd the bifurcating orbit will collide with an unstable sliding one on the boundary of the sliding region and disappear;

3. **Nonsmooth period-doubling:** if $\sigma_1^- + \sigma_2^-$ is odd, a period-doubling will be observed and the bifurcation will cause the formation of a sliding orbit with doubled period (with respect to bifurcating periodic solution).

In the case under investigation, the eigenvalues of A_1 in (39) are $\lambda_{11} = 0.0107$, $\lambda_{12} = 0.8433$ while those of A_2 are $\lambda_{21} = 0$, $\lambda_{22} = -1.8500$. Hence, $\sigma_1^+ + \sigma_2^+ = 0$ is even while $\sigma_1^- + \sigma_2^- = 1$ is odd. Therefore, according to the classification strategy presented in [33], at the grazing-sliding bifurcation point we will observe the transition from the non-sticking bifurcating orbit to two coexisting sliding solutions; an orbit sharing the same periodicity of the bifurcating one and a period-doubled periodic solution.

Moreover, since λ_{22} is outside of the unit circle, the sliding orbit born through the aforementioned smooth transition will be unstable. Similarly, as the eigenvalues of the second-iterate of map (39) also lie outside the unit circle, the nonsmooth period-doubling will give rise to an unstable orbit.

Hence, we can conclude that at the grazing-sliding, the bifurcating orbit will not persist. Namely, the transition will be observed from the stable $4T$-periodic solution (without any stick phase) to at least two coexisting unstable solutions: an unstable sliding orbit of period $4T$ and an unstable $8T$-periodic solutions.

Note that because of its applicability to general n-dimensional systems, the classification strategy above does not offer any information on the possible existence of aperiodic solutions or periodic orbits of periodicity higher than 2 past the bifurcation point. This must be checked *a posteriori* by using appropriate tools from nonlinear dynamics and is only feasible, as we write, for low-dimensional maps.

In our case, as the Poincaré map of the orbit under investigation is two-dimensional we can gather this extra information by using the classification of border-collisions in two-dimensional piecewise-linear maps recently presented in [14, 34]. Briefly, this strategy consists of a set of inequalities involving the trace and the determinant of the map matrices on both sides of the boundary. Here, we present only the final results. For a more detailed description of the method, we refer the reader to [34].

Following, [14, 34] we calculate the appropriate quantities and find that they satisfy the following inequality:

1. $2\sqrt{\delta_L} < \tau_L < (1 + \delta_L)$,
2. $\tau_R < -(1 + \delta_R)$,

where $\delta_1 = \lambda_{11}\lambda_{12} = 0.009$, $\delta_2 = \lambda_{21}\lambda_{22} = 0$, $\tau_1 = \lambda_{11} + \lambda_{12} = 0.8540$, $\tau_2 = \lambda_{21} + \lambda_{22} = -1.85$ are the determinants and traces of the map matrices A_1 and A_2 on both sides of the boundary. As shown in in [34], this implies that a chaotic attractor will be coexisting with the unstable orbits detected above past the grazing-sliding bifurcation point.

Hence, the numerical results reported in [13] and depicted in Fig.7 are confirmed and explained analytically, confirming the role of grazing-sliding in causing the trasition from periodic non-sticking solutions to fully blown chaotic stick-slip motion.

6 Conclusions

It was shown that a novel class of bifurcations, so-called sliding bifurcations, play an important role in dry friction oscillators. Normal form maps (discontinuity maps) describing these bifurcations have been introduced. This normal form maps allow us the derivation of the Poincaré

map describing the system behaviour close to the bifurcation point. This map can then be used to classify hence predict analytically the scenarios following a sliding bifurcation.

A dry friction oscillator, recently reported in the literature, has been used as an illustrative example and analysed from the standpoint of sliding bifurcation theory. It has been shown that the bifurcation of a periodic orbit leading to the onset of chaotic motion (reported in [13]), accompanied by slip to stick-slip transition, can be explained in terms of a grazing-sliding bifurcation. Detailed analysis shows how the grazing sliding bifurcation translates into a piecewise linear Poincaré map (PWL) describing the system dynamics close to the bifurcation point. Thus, the conjecture, often made in the literature, that bifurcations in friction oscillator correspond to so-called border-collisions of piecewise linear maps, has been rigorously proven and linked to the occurrence of grazing-sliding bifurcations of the corresponding flow.

We wish to emphasize that only in this case, the classification schemes developed for border-collision in PWL maps ([33, 34]) can be used to predict the dynamical scenario following the bifurcation. Their application was reported to the friction oscillator under investigation. It was shown that the route to chaos in this system is associated to a grazing-sliding bifurcation causing the sudden appearance of chaotic stick-slip motion.

We anticipate that sliding bifurcations are bound to be a common feature in friction systems and more generally vibro-impacting mechanical systems. The approach described in this paper can then be used effectively to explain the occurrence of complex behaviour and predict unwanted dynamics.

Further work will be directed towards the analysis of other types of sliding bifurcations in friction oscillators and other systems of relevance in applications, with particular attention to higher-dimensional systems. A pressing open problem is the classification of border-collisions in maps which are locally piecewise-smooth but not piecewise-linear.

References

[1] J.P. Hartog. Forced vibrations with combined columb and viscous friction. *Transaction of the American Society of Mechanical Engineering*, 53:107 – 115, 1931.

[2] A. A. Andronov, S. E. Khaikin, and A. A. Vitt. *Theory of Oscillators.* Pergamon Press, Oxford, 1965.

[3] T.K. Pratt and R.Williams. Non-linear analysis for stick-slip motion. *Journal of Sound and Vibration*, 74:531 – 542, 1981.

[4] K. Popp and P. Shelter. Stick–slip vibrations and chaos. *Philosophical Transactions of the Royal Society A*, 332(1624):89–105, 1990.

[5] P. Stelter. Non-linear vibrations of structures induced by dry friction. *Nonlinear Dynamics*, 3:329 – 345, 1992.

[6] K. Popp, N. Hinrichs, and M. Oestreich. Dynamical behaviour of friction oscillators with simultaneous self and external excitation. *Sadhana (Indian Academy of Sciences)*, 20:627–654, 1995.

[7] M. Oestreich N. Hinrichs and K. Popp. On the modelling of friction oscillators. *Journal of Sound and Vibration*, 216(3):435–459, 1998.

[8] S. R. Bishop U. Galvanetto. Computational techniques for nonlinear dynamics in multiple frictionoscillators. *Computer methods in applied mechanics and engineering*, 163:373 – 382, 1998.

[9] U. Galvanetto. Bifurcations and chaos in a four-dimensional mechanical system with dry-friction. *Journal of Sound and Vibration*, 204(4):690 – 695, 1997.

[10] U. Galvanetto. Some discontinuous bifurcations in a two block stick-slip system. *Computer methods in applied mechanics and engineering*, 178:291 – 306, 1998.

[11] U. Galvanetto. Some discontinuous bifurcations in a two block stick-slip system. *Journal of Sound and Vibration*, 284(4):653 – 669, 2001.

[12] U. Galvanetto and S.R. Bishop. Dynamics of a simple damped oscillator undergoing stick-slip vibrations. *Meccanica*, 178:291 – 306, 1998.

[13] Y. Yoshitake and A. Sueoka. *Applied nonlinear dynamics and chaos of mechanical systems with discontinuities*, chapter Forced Self-Excited Vibration with Dry Friction. World Scientific, 2000.

[14] H. E. Nusse and J. A. Yorke. Border–collision bifurcations for piece-wise smooth one-dimensional maps. *International Journal of Bifurcation and Chaos*, 5:189–207, 1995.

[15] H. E. Nusse and J. A. Yorke. Border-collision bifurcations including 'period two to period three' for piecewise smooth systems. *Physica D*, 57:39–57, 1992.

[16] H. E. Nusse and J. A. Yorke. Border collision bifurcation: an explanation for observed bifurcation phenomena. *Physical Review E*, 49:1073–1076, 1994.

[17] G. Yuan, S. Banerjee, E Ott, and J.A. Yorke. Border-collision bifurcations in the buck converter. *IEEE Transactions on Circuits and Systems–I*, 45:707–716, 1998.

[18] M. di Bernardo, A. R. Champneys, F. Garofalo, L. Glielmo, and F. Vasca. Nonlinear phenomena in closed loop DC/DC buck converter. *Proceedings NDES96 (Nonlinear Dynamics in Electronic Systems*, 1:51–56, 1996.

[19] M. di Bernardo, F. Garofalo, L. Glielmo, and F. Vasca. Switchings, bifurcations and chaos in DC/DC converters. *IEEE Transactions on Circuits and Systems, Part I*, 45:133–141, 1998.

[20] M. di Bernardo, A. R. Champneys, and C. J. Budd. Grazing, skipping and sliding: analysis of the nonsmooth dynamics of the DC/DC buck converter. *Nonlinearity*, 11:858–890, 1998.

[21] B. Brogliato. *Nonsmooth Mechanics*. Springer–Verlag, 1999.

[22] M. di Bernardo, C.J. Budd, and A.R. Champneys. Unified framework for the analysis of grazing and border-collisions in piecewise-smooth systems. *Physical Review Letters*, 86(12):2554–2556, 2001.

[23] M. di Bernardo, C.J. Budd, and A. R. Champneys. Corner–collision implies border–collision bifurcation. *Physica D*, 154:171 – 194, 2001.

[24] M. I. Feigin. *Forced Oscillations in systems with discontinuous nonlinearities.* Nauka, Moscow, 1994. In Russian.

[25] M. di Bernardo, K.H. Johansson, and F. Vasca. Self-oscillations in relay feedback systems: Symmetry and bifurcations. *International Journal of Bifurcations and Chaos*, (4), 2001.

[26] S.W. Shaw. On the dynamic response of a system with dry friction. *Journal of Sound and Vibration*, 108(2):305–325, 1986.

[27] A.F. Filippov. *Differential equations with discontinuous righthand sides.* Kluwer, Dortrecht, 1988.

[28] V. I. Utkin. *Sliding Modes in Control Optimization.* Springer-Verlag, Berlin, 1992.

[29] P. Kowalczyk and M. di Bernardo. On a novel class of bifurcations in hybrid dynamical systems - the case of relay feedback systems. In *Proceeding of Hybrid Systems Computation and Control*, pages 361–374. Springer–Verlag, 2001.

[30] M. di Bernardo, P.Kowalczyk, and A.Nordmark. Bifurcations of dynamical systems with sliding: derivation of normal form mappings. accepted for publication in Physica D, 2002.

[31] Y.A. Kuznetsov. *Elements of Applied Bifurcation Theory.* Springer-Verlag, 1995.

[32] A. B. Nordmark. Non-periodic motion caused by grazing incidence in impact oscillators. *Journal of Sound and Vibration*, 2:279–297, 1991.

[33] M. di Bernardo, M.I. Feigin, S.J. Hogan, and M.E. Homer. Local analysis of C-bifurcations in n-dimensional piecewise smooth dynamical systems. *Chaos, Solitons and Fractals*, 10:1881–1908, 1999.

[34] S. Banerjee and C. Grebogi. Border collision bifurcations in two-dimensional piecewise smooth maps. *Physical Review E*, 59:4052–4061, 1999.